

B-3-6

# InP-Based Quantum Cascade Lateral Grating Distributed Feedback Lasers

K. Kennedy<sup>1</sup>, D. G. Revin<sup>2</sup>, A. B. Krysa<sup>1</sup>, K. M. Groom<sup>1</sup>, L. R. Wilson<sup>2</sup>, J. W. Cockburn<sup>2</sup>, R. A. Hogg<sup>1</sup>

1 -EPSRC National Centre for III-V Technologies, University of Sheffield, Sir Frederick Mappin Building, Sheffield, S1 3JD, UK

2- University of Sheffield, Department of Physics and Astronomy, Sheffield S3 7RH, UK

E-mail: [k.kennedy@sheffield.ac.uk](mailto:k.kennedy@sheffield.ac.uk)

**Abstract** – We report device results and techniques for fabricating gratings for InP-based quantum cascade (DFB) lasers, grown by MOVPE. Deeply etched lateral gratings are achieved by the development of a novel two-stage ICP etch process.

## I. INTRODUCTION

The realisation of quantum cascade distributed feedback (QCDFB) lasers<sup>[1][2]</sup> as a cost effective, powerful, single mode laser source in the mid-infrared (MIR) has created many real world applications. Recent improvements in quantum cascade laser performance have made them a suitable alternative to gas lasers in applications such as high resolution, trace gas sensing and spectroscopy<sup>[3][4]</sup>. A number of applications require single mode emission when operating near room temperature with the ability to tune the wavelength continuously over a large range. The conventional method of tuning the QC laser wavelength is to vary the operating temperature with typical tuning coefficients of approximately  $-0.07\text{cm}^{-1}/\text{K}$ <sup>[5][6]</sup>. We report the single mode operation of InP-based quantum cascade distributed feedback (QCDFB) lasers with AlInAs / InGaAs active regions, below and above room temperature. The material was grown by MOVPE and the structure is based on a double-phonon resonance design<sup>[7]</sup>, with a four well active region structure. More details on this 35 active region structure, including the layer thicknesses, is given in previous publications<sup>[5][8]</sup>. Typically, QCDFB devices have a grating etched into the top of the laser waveguide<sup>[1]</sup>, partially removing the top plasmon-confining layer. This design relies on a portion of the optical mode interacting with the metal in the grating resulting in a localised loss. Crucially, the loss component helps lift the degeneracy between the two modes on either side of the stop-band<sup>[9]</sup>. Although effective, this method requires the grating and laser ridge to be fabricated in two distinct steps. By monolithically fabricating the lateral gratings simultaneously with the ridge<sup>[10]</sup> we significantly reduce process time and cost. Additionally, the top of the ridge is left planar by moving the grating to the side and deep Bragg mirrors<sup>[11]</sup> could be used. In this paper, we report the first realization of InP based lateral grating DFBs with high performance, made possible by the development of a two-stage inductively coupled plasma (ICP) etch process.

## II. SAMPLE GROWTH AND FABRICATION

The AlInAs / InGaAs active region and the doped InP waveguide have appreciably different etch rates and surface morphology for certain etch chemistries and so the

development of a high aspect ratio, two-stage, ICP etch process was required before the realisation of these devices was possible. To achieve a smooth, vertical corrugation of the active region the etch depth was required to be  $10\mu\text{m}$  or more. To achieve such a depth the etch selectivity needs to be high and so a dielectric mask, silicon dioxide ( $\text{SiO}_2$ ), was favoured. The  $\text{SiO}_2$  layer (thickness =  $800\text{nm}$ ) was deposited by plasma enhanced chemical vapour deposition (PECVD). After spin coating the sample with SPR350 photoresist, conventional contact lithography (UV300) was employed to pattern the sample with the rib waveguide (grating period,  $\Lambda = 1.68\mu\text{m}$ ). After development of the photoresist the pattern was transferred into the  $\text{SiO}_2$  layer by using an Oxford Instruments Plasmalab System 100 ICP etcher. Using a  $\text{CHF}_3/\text{Ar}$  chemistry (rf power =  $200\text{W}$ ), the process was optimised to gain a smooth vertical etch profile and a photoresist to  $\text{SiO}_2$  selectivity of  $\sim 1:4$ . After the dielectric etch was complete the remaining photoresist on the sample was removed using an oxygen plasma ash ready for the semiconductor etch in the ICP etcher. Initial trials using InP substrates were successfully etched in a  $\text{Cl}_2/\text{Ar}$  atmosphere achieving smooth vertical etching and good etch selectivity. However, when the process was transferred on to the full QCL structure the vertical etching and good definition of the rib structure was lost. This was due to the different etching rates of the InP waveguide and the active region materials. A similar etch rate between the different layers and a good morphology was obtained by switching to a  $\text{SiCl}_4/\text{Ar}$  atmosphere but an excessive amount of mask etching reduced the selectivity and some undercutting of the mask was evident. This initiated the development of a two-stage etch process utilising the two different etch chemistries. The result was a high aspect ratio etch with a smooth vertical etch profile and a suitable etch rate. The final process incorporated two etches using  $\text{Cl}_2/\text{Ar}$  (etch rate =  $430\text{nm}/\text{min}$ ) followed by an etch using  $\text{SiCl}_4/\text{Ar}$  (etch rate =  $1\mu\text{m}/\text{min}$ ). The chamber pressure was  $2\text{mTorr}$  and table temperature was  $25^\circ\text{C}$ . The rf powers / ICP powers were  $300\text{W}/500\text{W}$  and  $220\text{W}/1000\text{W}$  respectively. The total etch time including the pump down was 23 minutes and a semiconductor to mask etch selectivity  $>15:1$  was achieved. The remaining dielectric mask was removed and then a dielectric layer was deposited by PECVD for electrical isolation. The contact window was opened in the dielectric layer using a reactive ion etch (RIE) and Ti/Au electrical contacts were thermally evaporated onto the sample

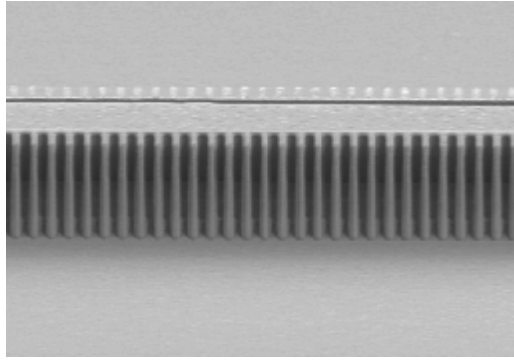


Fig. 1. Scanning electron microscope image of a quantum cascade DFB laser ridge with deeply etched lateral gratings. The sample is shown after metallization after a dielectric layer was deposited by PECVD and a contact window opened by reactive ion etching.

as shown in Fig. 1. Finally,  $\sim 1\mu\text{m}$  of electroplated gold was deposited on the sample.

### III. RESULTS AND DISCUSSION

Fabry-Perot (FP) lasers were simultaneously fabricated on the sample with the DFB devices. The DFB ridge widths were the same as for the FPs but the additional rib structures were either  $1\mu\text{m}$ ,  $3\mu\text{m}$  or  $5\mu\text{m}$  wide. This allowed the direct comparison of the DFB designs with their corresponding FP devices. Several un-coated devices were mounted on copper blocks, gold wire bonded and tested using an electrical pulse length of 25ns and repetition rate of 5kHz. The device emission spectra were measured using a Fourier Transform Infra-Red (FTIR) spectrometer with a resolution of  $0.2\text{cm}^{-1}$ . Single mode laser emission (linewidth  $\sim 0.3\text{cm}^{-1}$ ) was measured for the DFB devices operating at room temperature and this was still the case when operating at well above threshold. For the  $9\mu\text{m}$  ( $\lambda \sim 9.91\mu\text{m}$ ) and  $14\mu\text{m}$  ( $\lambda \sim 10.1\mu\text{m}$ ) wide ridges, the effective refractive index ( $n_{\text{eff}}$ ) =  $\lambda / 2\Lambda$  was calculated to be ( $\approx 2.95$ ) and ( $\approx 2.99$ ) respectively at room temperature. Further emission spectra measurements were carried out on two devices with length = 0.65mm. The ridge widths were  $9\mu\text{m}$  ( $N_3$ ) and  $14\mu\text{m}$  ( $W_1$ ) and the rib widths were  $3\mu\text{m}$  and  $1\mu\text{m}$  respectively. For both devices the observed change in wavelength over a temperature range of 190K to 330K is linear, with a tuning coefficient measured to be  $-0.067\text{cm}^{-1}\text{K}^{-1}$ . In (Fig. 2) the emission spectra also shows the dependence of the wavelength on the ridge width ( $w$ ), giving ( $dv/dw \approx 3\text{cm}^{-1}/\mu\text{m}$ ). The side mode suppression ratio (SMSR) for  $N_3$  was greater than 30dB for temperatures higher than 190K where no other side modes were present. The SMSR for  $W_1$  was  $>18\text{dB}$  at room temperature and above. The inferior single mode performance of  $W_1$  compared to  $N_3$  is attributed to the reduced coupling coefficient, which is caused by the smaller rib length and wider ridge width. Additionally, a 0.95mm long DFB with a  $14\mu\text{m}$  wide ridge,  $5\mu\text{m}$  rib width and as-cleaved facets was measured as having

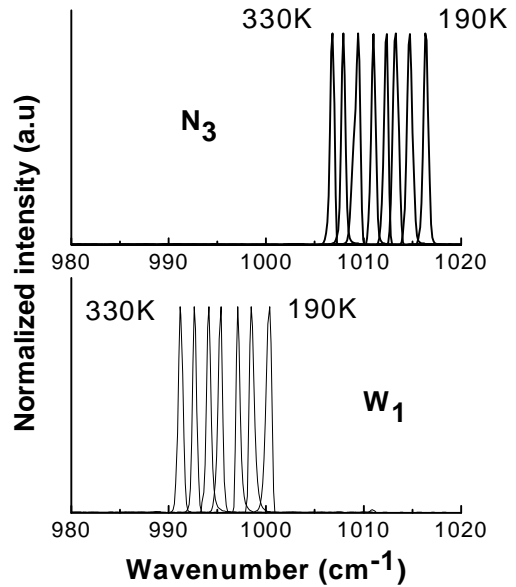


Fig. 2. Single-mode Laser emission spectra measured close to threshold over a range of temperatures between 190K and 330K for devices  $N_3$  and  $W_1$ . Pulsing conditions used were 25ns pulse width at a 5kHz repetition rate.

single-mode emission (SMSR  $>30\text{dB}$ ) with peak optical output power up to  $\sim 30\text{mW}$  at room temperature. The threshold current densities and (slope efficiencies) at 293K were  $\sim 5.5\text{ kA/cm}^2$  ( $\sim 64\text{mW/A}$ ) and at 250K they were  $\sim 4.3\text{ kA/cm}^2$  ( $\sim 85\text{mW/A}$ ).

### ACKNOWLEDGMENT

The authors gratefully acknowledge the assistance of the staff at the EPSRC National Centre for III-V Technologies, Sheffield.

### REFERENCES

- [1] J. Faist, C. Gmachl, F. Capasso, C. Sirtori, et al, Appl. Phys. Lett. **70**, 20, 2670-2672 (1997)
- [2] C. Gmachl, J. Faist, J.N. Baillargeon, F. Capasso, C. Sirtori, et al, IEEE. Phot. Tech. Lett. **9**, 1090-1092 (1997)
- [3] C. Gmachl, F. Capasso, D. L. Sivco, A. Y. Cho, Rep. Prog. Phys. **64**, 1533 (2001)
- [4] R. Kohler, C. Gmachl, F. Capasso, et al, IEEE Phot. Lett. Vol.12, no.5, 1041, May (2000)
- [5] R. P. Green, L.R. Wilson, E.A. Zibik, D.G. Revin, J. W. Cockburn et al, Appl. Phys. Lett. **85**, 5529 (2004)
- [6] D. Hofstetter, J. Faist, M. Beck, A. Muller, U. Oesterle App. Phys. Lett. **75**, 665 (1999)
- [7] M. Beck, D. Hofstetter, T. Aellen, J. Faist, U. Oesterle, M. Illegems, E.Gini, and H. Melchior, Science **295**, 301 (2002)
- [8] A.B. Krysa, J.S. Roberts, R.P. Green, L.R. Wilson, H. Page, M. Garcia, J.W. Cockburn, J. of Crystal Growth, **272**, 682-685, (2004)
- [9] Kogelnik and C. Shank, J. Appl. Phys 43, 2327 (1972)
- [10] S. Golka, C. Pflugl, W. Shrenk, G. Strasser, App. Phys. Lett. **86**, 111103 (2005)
- [11] S. Hofling, J.P. Reithmaier, A.Forchel, IEEE J. of Sel. Top. in Quant. Elect. **11**, 5, 1048-1054 (2005)